第26回橋梁等の耐震設計シンポジウム
講演論文集（2023年7月）

Changes in Vibration Characteristic of Bridge System with Progress of Local Scouring

Takahiro Iwata[1]・Ricky Chan[2]・Koji Kinoshita[3]

[1] Student Member of JSCE, Department of Civil and Environmental Engineering, Gifu University
(1-1 Yanagido,Gifu City 501-1193, Japan)
[2]Associate Professor, School of Engineering, RMIT University (124 La Trobe Street, Melbourne VIC 3000, Aust
[3]Member of JSCE, Associate Professor, Department of Civil Engineering, Gifu University
(1-1 Yanagido,Gifu City 501-1193, Japan)

1. Introduction

Bridge scouring refers to the process of erosion and removal of sediment, such as sand, gravel, and rocks, from around bridge foundations or piers by flowing water, particularly in rivers and streams. Bridge scouring is a widespread and ongoing problem that has significant consequences for public safety and infrastructure. Bridge failures caused by scouring may lead to loss of life, economic costs, and severe property damage. Scouring accounts for half of all highway bridge failures in the United States [1)]. Following damage for bridge due to the scouring, the National Bridge Inspection Standards were established in the United States to prevent similar disasters [2)]. Despite these measures, the problem of bridge scouring persists, and with the increasing frequency and severity of extreme weather events associated with climate change, it is expected to worsen.

Several methods can be employed to mitigate the risk of bridge scouring, including the use of erosion-resistant materials for bridge foundations, the installation of protective measures, and conducting regular inspections and maintenance. Traditionally, inspections of scouring are carried out by divers or underwater drones to visually inspect the scouring conditions up close or indirectly, or by using embedded poles to identify riverbed fluctuations. However, visually assessing the situation can be challenging because scouring occurs particularly during rainfall with raised river levels and increased flow rates resulting in the scouring of the ground.

The objective of this study was to investigate the impact of local scouring on the vibration characteristics of bridges. Specifically, changes in vibration characteristics were investigated by reduced model tests and numerical analyses based on these tests, in which local scouring was simulated by excavating the ground around direct foundations with different dimensions of pile foundations and footings.

2. Investigation using single-column specimens

In previous studies, the focus has mainly been on changes in the natural frequencies of bridge columns due to scouring [3-6)]. However, most of these studies have utilized single-column specimens without footings, which may not represent the actual bridge conditions accurately. Therefore, in this chapter, the objective is to conduct experimental and analytical investigations using small-scale single-column specimens that incorporate various foundation types.

(1) Details of experiments

Fig. 1 shows the testing setup and specimens utilized in this study. Four types of specimens were used, classified as either spread foundation specimens or pile foundation specimens. The spread foundation specimens consisted of footings with widths of 150 mm squares or 100 mm squares, while some had no footings at all. On the other hand, the pile foundation specimen was made up of a 200

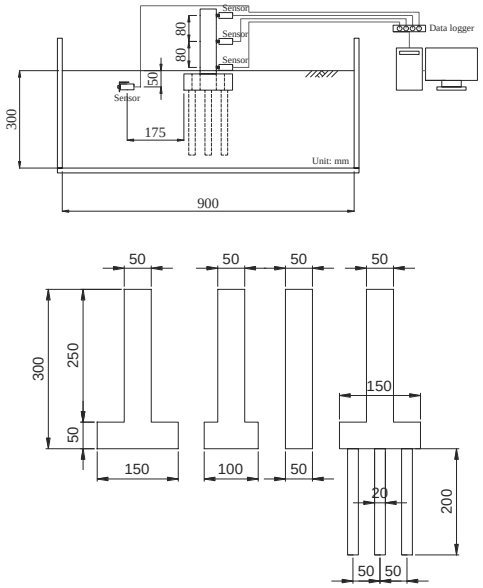


Fig. 1 Experimental setup

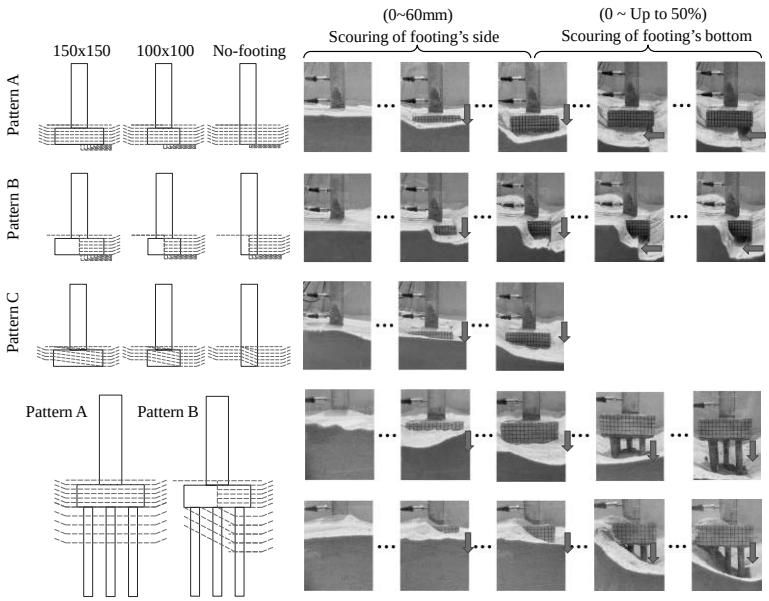


Fig. 2 Experimental step

mm length steel pipe pile. Specifically, the diameter of the steel pipe was 20 mm, and the thickness was 1 mm. The columns and footings of the specimens were constructed using mortar and reinforced with steel mesh. The specimens were placed in a sand box with dimensions of 900 mm in length, 400 mm in width, and 300 mm in height. To measure the vibration data, three acceleration sensors were attached to the columns at 80 mm intervals, and one acceleration sensor was placed in the subgrade. The detail of the acceleration sensor, the sensitivity was 100 mV/g, the frequency range was 2048 Hz, and the measurement range was 50 g. The average particle diameter D_{50} was found to be 1 mm from sieve analysis.

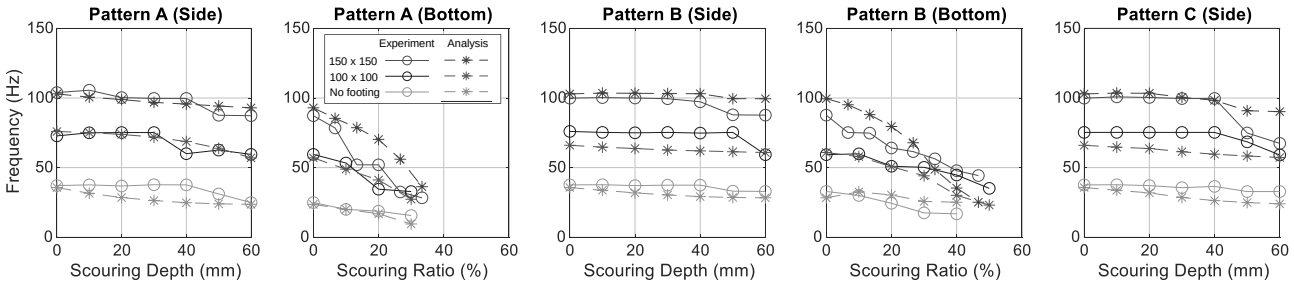
Fig. 2 shows the testing procedures used to evaluate side and bottom scouring. Side scouring refers to a maximum scouring depth of 60 mm, where 0 mm corresponds to no scouring. Bottom scouring was characterized by the ratio of scouring length to footing width, with scouring rates varying from 0% to a maximum of 50%. In the spread foundation specimens, three patterns of scouring were considered and carried out: Pattern A, which involved uniform scouring; Pattern B, which involved scouring on one side only; and Pattern C, which involved diagonal scouring. Meanwhile, in the pile foundation specimens, two patterns of scouring were considered and carried out: Pattern A, which was the same as the uniform scouring in the spread foundation specimens, and Pattern B, which involved scouring on one side only. However, in Pattern B at the bottom scouring of the pile foundation, the bottom scouring was oblique.

Two types of vibration were investigated during the testing phase: hammer testing, which involved measuring free vibration by applying an impact force using a modal hammer, and micro-tremor testing, which involved measuring free vibration caused by environmental vibrations. The vibration data collected during each experiment was transformed into the frequency domain using Fast Fourier Transform (FFT), and the power spectrum density was calculated. However, in the case of micro-tremor testing, it will be difficult to find true modal frequency from these results because the subgrade vibration characteristics were included in the FFT results. Therefore, a Frequency Response Function (FRF) was calculated to remove the subgrade vibration characteristics [7, 8].

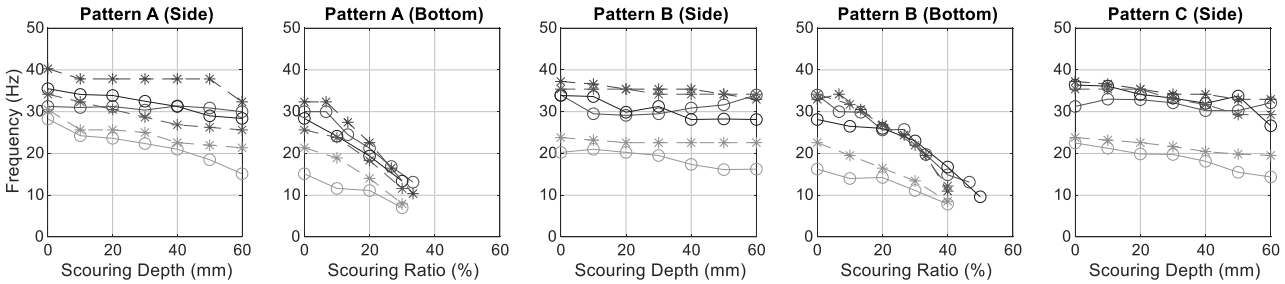
(2) Experimental results

Fig. 3 presents the testing results, which include charts showing the relationship between the natural frequency and scouring depth or the ratio of scouring length or depth. These plots were obtained from a series of calculations, including the FFT. **Fig. 3** also includes the results of the analysis described below.

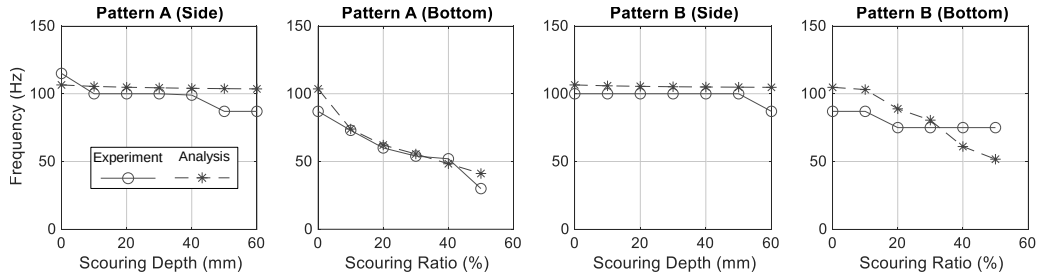
As for micro-tremors testing results on side scouring of pattern A, it can be observed that the natural frequency of each type of specimen began to decrease at scouring depths of 30 to 40 mm. In addition, for the bottom scouring testing, it was found that the larger the footing, which is such as a



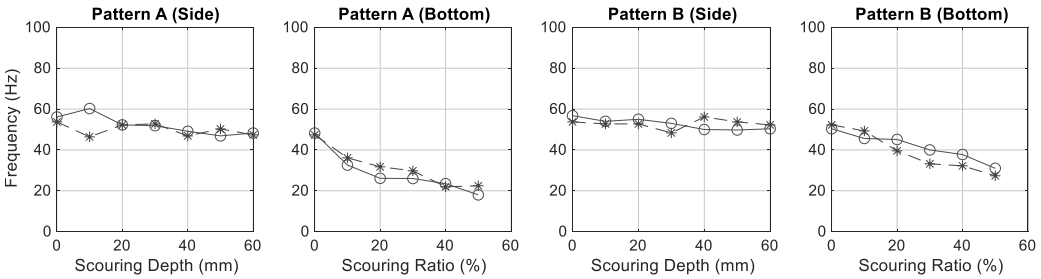
(a) Micro-tremors testing results of spread foundations



(b) Hammer testing results of spread foundations



(c) Micro-tremors testing results of pile foundations



(d) Hammer testing results of pile foundations

Fig. 3 Experimental and analytical results of single-column specimens

150 mm squares specimen, the more significant the decrease in natural frequencies due to bottom scouring from the results. In the case of the pile foundation testing, the decrease of the natural frequency began at scouring depth of 40 to 50 mm on side scouring. Also, in the bottom scouring, the natural frequencies were reduced by up to approximately 70 %. For the side scouring of pattern B, it was found that the natural frequency of each specimen began to decrease at scouring depths of 40 to 50 mm. Moreover, in the bottom scouring tests, the results showed a slower downward trend compared to Pattern A. This behavior can be attributed to the higher subgrade restraint in the case of Pattern B, which involves one-sided scouring, compared to Pattern A, which involves uniform scouring. For pattern C, it was found that the natural frequency of each type of specimen began to decrease at a scouring depth of 40 mm, and the decrease ratio is similar to Pattern A result. In the pile foundation specimen, the natural frequency began to decrease at a scouring depth of 50 to 60 mm. At the bottom scouring, the natural frequency decreased slightly but then remained almost constant.

On the other hand, regarding the hammer testing results, it was found that for the Pattern A, the natural frequency of the 100 mm square specimen with no footing began to

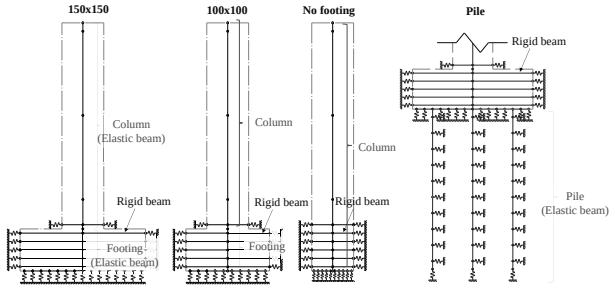


Fig. 4 Analytical models of specimens

decrease from the beginning. In contrast, the natural frequency of the 150 mm square specimen showed no significant change. This behavior is attributed to the small variations of impact forces under laboratory conditions. As a result, the natural frequencies of the 100 mm square specimens were sometimes higher than those of the 150 mm square specimens. Furthermore, the results of the bottom scouring tests also exhibited a similar trend as the micro-tremors testing, where the larger the footing, the greater the reduction in natural frequencies. As for the pile foundation specimen, the natural frequency was reduced by up to approximately 60 %. In the case of pattern B, the decreasing trend of natural frequency is slower than that of Pattern A, as observed in the constant microtremor tests. Also, pattern C exhibits a trend that is approximately midway between Pattern A and Pattern B.

From the above, testing of single-column specimens showed that the natural frequency decreases due to bridge scouring in each case, as evidenced by both micro-tremor and hammer testing. Moreover, in Pattern B, there is a delay in the decrease of natural frequency compared to pattern A because the subgrade reaction is larger.

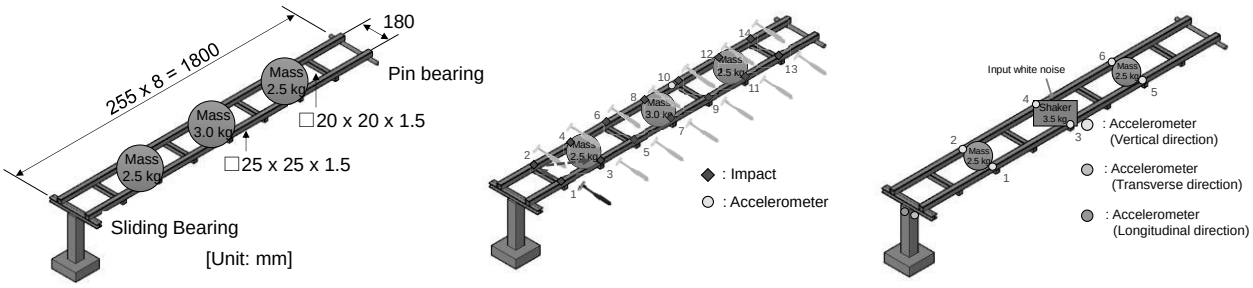
(3) Analytical model

Fig. 4 shows analytical models for both spread foundation specimens and pile foundation specimens. In the spread foundation models, the columns and footings were modeled using elastic beam elements, and Young's modulus was set to 28,000 MPa. Additionally, the density of mortar was assumed to be 2.0 ton/m^3. The subgrade conditions were modeled using spring elements, and each spring element was connected to the footing element by an elastic beam element, which served as an offset member. The values of the subgrade conditions were calculated based on Specifications for Highway Bridges [9]. The details of equations are omitted for reasons of space limitation. In the pile foundation model, the element was represented as an elastic beam, and Young's modulus was set to 200,000 MPa. In this analysis, acceleration data was input to each element, and the corresponding response acceleration was calculated. The input acceleration was white noise for micro-tremors. Also, as for the hammer testing, its impact acceleration with the maximum acceleration obtained from testing results. Subsequently, the natural frequency was determined using FFT.

(4) Analytical results

Fig. 3 shows the analytical results compared to the testing results. In the case of micro-tremor testing on pattern A with side scouring, the analytical results for the 150 mm and 100 mm square footing models agreed with the testing results, and the margin of error was within 10%. For the no-footing models, the decreasing trend of the natural frequencies was different, but the natural frequency at scouring depths of 0 and 60 mm were identical. In the bottom scouring, the decreasing trend of the natural frequency was different in the 150 mm square footing specimen. However, results of 100 mm square footing and no-footing model were agreed with the testing results. In the case of pattern B and C with the side scouring, the results of the 150 mm square footing model at side scouring agree with the testing results. However, the results of the 100 mm squares and no-footing models showed errors of about 15%. Nevertheless, the decreasing trend in each model was almost similar to the testing results. Additionally, in the case of bottom scouring, the decreasing trend of the 150 mm square footing model differed slightly from the testing results, while the 100 mm square footing and no-footing models almost agreed with the testing results. As for the pile foundation model, the results were almost consistent with the testing results. These results suggest that it is possible to evaluate the natural frequencies during the micro-tremors using the analytical models tested.

On the other hand, in the case of the hummer testing conducted on pattern A, the 150 mm square footing model did not produce results that agreed with the testing results, while other models did. However, when it came to bottom scouring, the analytical results were mostly consistent with the testing results. In the case of patterns B and C, analytical results from each model were mostly consistent with the experimental results. The analysis results of the hammer testing suggest that the non-linear behaviors of the scoured bridge were able to be evaluated using these models.



(a) Detail (b) Roving hammer tests (c) Shaking tests

Fig. 5 Experimental setup for specimens with superstructure

3. Investigation using bridge system specimens

In practical field conditions, instrumentation on bridge piers may be difficult due to access difficulties including the use of elevated platforms or scaffolds. Thus, in this section, we investigate the potential changes in vibrational characteristics on bridge superstructure (i.e., bridge deck) due to scouring in the foundation If scouring causes changes in the vibration characteristics of the substructure, it is expected that the vibration characteristics of the superstructure will also change accordingly. By detecting scouring through changes in the vibration characteristics of the superstructure, it would be easier to install acceleration sensors and other monitoring equipment. Therefore, this chapter focuses on conducting scouring experiments that include the superstructure, in order to investigate the changes in the vibration characteristics of the entire bridge system caused by scouring.

(1) Detail of experimental setup

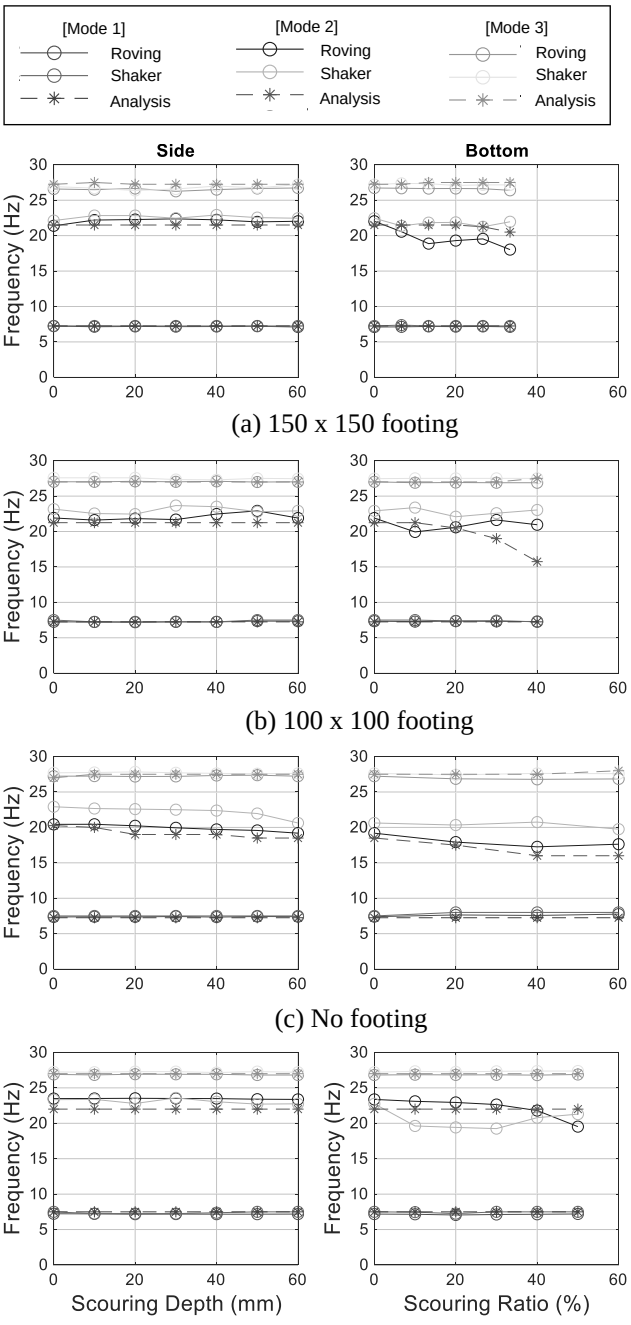
Fig. 5 shows the experimental setup for bridge system specimens. The superstructure is constructed using aluminum steel beams. The main beam, oriented in the longitudinal direction, has a length of 1800 mm and is made from 25 mm square hollow sections with a thickness of 1.5 mm. The width of the superstructure measures 180 mm and employs 20 mm square hollow sections with a thickness of 1.5 mm. To address the challenge of obtaining sufficient vibration data due to the lightweight nature of the aluminum superstructure, additional masses totaling 8 kg were incorporated. Out of this, 3 kg accounts for the weight of the exciters utilized in the shaker experiments. The testing was focused on investigating the effects of uniform scouring only and considering transverse scouring in the case of bottom scouring. That is mean the same with Pattern A in Section 2 experiment.

The focus of the investigation is on the changes in the vibration characteristics of the superstructure, specifically the natural frequencies and eigenmodes. To measure the vibration data of the bridge system, two types of testing were conducted. First, a roving hammer test, which involved one fixed accelerometer and one roving modal hammer. The modal hammer was struck at each point where the eigenmode vector needed to be measured, and FRF was calculated using the input data from the modal hammer and the output data from the accelerometer. The eigenmodes can be determined from the peak plot of the imaginary part of the FRF. The second test is shaking. In this test, white noise vibrations were generated on a modal exciter to produce vibrations throughout the entire bridge system. Six accelerometers were installed on the superstructure, and two accelerometers were placed on the substructure to capture acceleration data. In this particular test, the vibration characteristics were calculated solely based on the output data obtained from the accelerometers. Although there are various methods available for calculating eigenfrequencies and eigenmodes using output data only, in this study, the Eigenvalue Realization Algorithm (ERA) was utilized. ERA is a widely used modal parameter estimation technique that can extract the eigenfrequencies and corresponding mode shapes from the measured response data of a structure [10].

(2) Experimental results

a) Superstructure

The results of the natural frequency analysis of the superstructure are shown in **Fig. 6**, and it also includes the results of the analysis described below. During the roving hammer testing, it was observed that only in Mode 2, the natural frequency decreased by approximately 20 to 25% at the bottom scouring in each specimen. Additionally, the specimen without a footing exhibited a 5% decrease in natural frequency at the side scouring. However, the natural frequencies of Mode 1 and Mode 3 remained



(a) 150 x 150 footing

(b) 100 x 100 footing

(c) No footing

(d) Pile

Fig. 6 Result of specimens with superstructure

largely unchanged.

In the shaking tests, the natural frequencies of Mode 2 were reduced by around 20% in the specimens without a footing and with piles. However, unlike the roving hammer testing, no reduction in natural frequencies was measured for the 150-square and 100-square specimens. This indicates that shaker testing, which only considers the output data to measure the natural vibrations and does not take into account the noise of the input components, is less accurate than roving hammer testing. However, in certain cases such as specimens without a footing and with piles, it is possible to detect a decrease in natural frequencies, and the accuracy of this detection depends on the condition of the foundation.

Tab. 1 shows the mode shapes of the superstructure for each specimen before and after scouring. Additionally, the table shows the Modal Assurance Criterion (MAC) values for end step compared to the initial state before scouring [11]. The MAC value represents the correlation between eigenmode vectors, with values closer to 1 indicating smaller changes and greater similarity between the compared modes. The results show that there is little change in the mode shape for each mode. Also, Mode 1 and Mode 3 were vertical modes, and Mode 2 was the torsional mode. The rotational mode around the axis significantly affects the vibration of the transverse component. Therefore, it can be concluded that the natural frequencies are indeed influenced by scouring in the transverse direction. The MAC results also indicate that although there are some partial errors in the data, most values are above 0.95, indicating that there is little change in the mode shape.

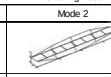
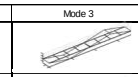
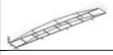
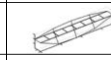
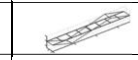
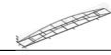
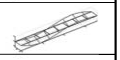
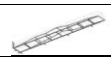
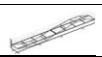
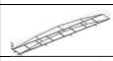
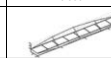
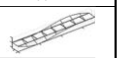
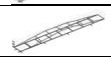
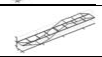
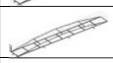
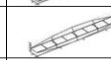
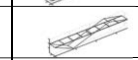
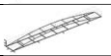
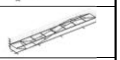
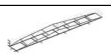
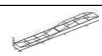
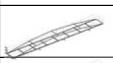
Based on the above results, it can be concluded that scouring reduces the natural frequency of the superstructure by up to 20% depending on the type of foundation, and that scouring can be detected by measuring the vibration data of the superstructure. Since there is little change in the mode shape, it is better to focus only on the natural frequencies for substructure.

b) Substructure

Fig. 7 shows the natural frequency results of the substructure. **Fig. 7** also includes the results of the analysis described below. It can be observed that the natural frequency in the transverse direction was changed in the 150-square and 100-square specimens. However, the natural frequency in the longitudinal direction remains unchanged and is identical to the mode 1 frequency of the superstructure.

Comparing the natural frequencies of the superstructure and substructure, it is evident from the results that the natural frequencies of the 150-square, 100-square specimens, and no footing specimens change in both the superstructure and substructure. However, only the pile specimen exhibit changes in natural frequencies. These results suggest that scouring may not be detected if measurements are carried out on only one of the structures. Therefore, it is advisable to observe and assess both the superstructure and the substructure in order to effectively detect scouring.

Tab. 1 Experimental and Analytical results of mode shape

		Roving Hammer Test			Shaking Test			Analysis		
		Mode 1	Mode 2	Mode 3	Mode 1	Mode 2	Mode 3	Mode 1	Mode 2	Mode 3
150 x 150 Footing	Initial									
	End									
	MAC	0.831	0.818	0.949	1.000	0.990	0.934	1.000	0.998	0.977
100 x 100 Footing	Initial									
	End									
	MAC	0.870	0.982	0.893	0.999	0.929	0.989	1.000	0.960	0.161
No footing	Initial									
	End									
	MAC	0.962	0.975	0.921	0.993	0.888	0.988	1.000	0.962	0.521
Pile	Initial									
	End									
	MAC	0.903	0.984	0.930	0.995	0.954	0.981	1.000	1.000	1.000

(3) Analytical investigations

a) Analytical model

Fig. 8 shows the analytical model for the specimen with the superstructure. The model includes spring elements to represent the bearings on the columns, taking into account the frictional stiffness between the superstructure and the column beams. Pin bearings are assumed for the bearings on the abutment side. In order to account for the effect of dead weight, a modal analysis alone is not sufficient. Therefore, the acceleration response data for each node was obtained by subjecting the structure to analysis with white noise excitation in three directions. The eigenfrequencies and eigenmodes were then obtained using the FRF method. The input data used for the FRF analysis is white noise.

b) Analytical results

Fig. 6 shows the results of the natural frequency of the superstructure. The natural frequencies in each mode and the changes in Mode 2 natural frequencies with scouring are reproduced to some extent in the analysis, but not with great accuracy. Additionally, **Tab. 1** shows the mode shapes of the superstructure for each specimen before and after scouring. Furthermore, the table shows the MAC values for each step compared to the initial state before scouring.

The analysis results clearly demonstrate a change in the eigenmodes in Mode 3 for the 100-square and No footing specimens, with the MAC value decreasing to 0.5 in the final step for the footing specimen. The natural frequency results also show analytically that the natural frequency of the torsional mode changes with scouring, although this may be due to the inaccuracy of the modeling of the test

(a) 150 x 150

(b) 100 x 100

(c) No footing

(d) Pile

Fig. 7 Results of substructure

Fig. 8 Analytical model for specimen with superstructure (Case: Pile specimen)

system.

Fig. 7 shows the natural frequency results obtained for the substructure. Comparing the variations in natural frequencies between the analytical and experimental approaches, it is evident that the analytical results generally exhibit a comparable degree of accuracy in capturing the natural frequencies and their corresponding variations as observed in the experimental results. This high level of agreement between the two methods indicates their effectiveness in accurately representing the dynamic behavior of the system under investigation. The utilization of these analytical models proves advantageous for conducting future parametric studies and case analyses involving factors such as ground conditions, bearing conditions, and other boundary conditions.

4. Conclusion

The objective of this study was to examine the effects of local scouring on the vibration characteristics of bridges. The conclusions of this research are summarized below:

[1] Experimental testing on single-column specimens revealed that bridge scouring leads to a decrease in natural frequency in all cases, as demonstrated by both micro-tremor and hammer testing. The natural frequencies exhibited reductions of up to 70%. This phenomenon was also observed in analytical models.

[2] The investigation using specimens with the superstructure indicated that scouring can be detected by examining changes in both the natural frequencies of the substructure and the natural frequencies of the superstructure. It was observed that the torsional mode shape about the bridge's longitudinal axis is changed, with the natural frequencies decreased by up to 20%.

[3] Focusing on either the superstructure or the substructure alone may result in the oversight of scouring. Therefore, it is recommended to carefully observe and evaluate both the superstructure and the substructure to ensure comprehensive detection of scouring.

Reference

1) Hunt BE. Monitoring scour critical bridges. Washington, D.C: Transportation Research Board; 2009.
2) Federal Highway Administration. National Bridge Inspection Standards, 2022.
3) Seki M, Tanaka H, Tsutsumi Y, Yamashita K, Nakano S, Nishimura A. A Proposal of Train Operation Control System of Railway Bridges Considering Natural Frequency of Piers Under Floods. Doboku Gakkai Ronbunshu, No. 686, VI-52, pp.78-89, 2001.
4) Prendergast LJ, Gavin K. A review of bridge scour monitoring techniques. Journal of Rock Mechanic and Geotechnical Engineering, Vol. 6, Issue 2, pp.138-149, 2014.
5) Ko YY, Lee WF, Chang WK, Mei HT, and Chen CH. Scour Evaluation of Bridge Foundations Using Vibration Measurement. Scour and Erosion, pp.884-893, 2010.
6) Naito N, Watanabe S, Keyaki T, Manome R, Nunokawa O. Vibration characteristics of spread foundation pier model with progress of local scouring. Japanese Geotechnical Journal, Vol. 15, Issue 2, pp.269-279, 2020.
7) Anders Brandt. Noise and Vibration Analysis: Signal Analysis and Experimental Procedures. John Wiley & Sons Ltd, 2011.
8) Vold, Havard, John Crowley, and G. Thomas Rocklin. New Ways of Estimating Frequency Response Functions. Sound and Vibration. Vol. 18, pp. 34–38, 1984.
9) Japan Road Association. SPECIFICATIONS FOR HIGHWAY BRIDGES. 2019.
10) Jer-Nan J., and Richard S.P. An Eigensystem Realization Algorithm for Modal Parameter Identification and Model Reduction. Journal of Guidance, Control, and Dynamics, Vol. 8, Issue. 5, 1985.
11) Miroslav P., Michal B., and Tomas H. Modal Assurance Criterion Procedia Engineering, Volume 48, pp.543-548, 2012.